On the Mechanism of Ehrlich Ascites Tumor Damage after Photodynamic Therapy

Živilė Lukšienė[1,4], Danutė Labeikytė[2], Audronė Marozienė[3], Regina Kliukienė[3], Narimantas Čėnas[3], Benediktas Juodka[2]

[1] *Lithuanian Oncology Center, Santariškių 1, LT-2600 Vilnius, Lithuania*
[2] *Vilnius University, M. K. Čiurlionio 21, LT- 2009 Vilnius, Lithuania*
[3] *Institute of Biochemistry, Mokslininku 12, LT-2600 Vilnius, Lithuania*
[4] *Institute of Materials Science and Applied Research, Saulėtekio 9, LT-2040 Vilnius, Lithuania*

Ehrlich ascites tumor damage after photodynamic treatment was investigated. According to the data obtained, HPde-PDT induces rapid cell membrane disintegration (blebbing, swelling), decrease in glutathione-S-transferase and DT-diaphorase activities, inhibition of DNA synthesis ([^{3}H Thy] incorporation), arrest of cell cycle in S and G_2M phases followed by apoptosis or necrosis. Due to the plethora of the above-mentioned injuries, Ehrlich ascites tumor growth was totally inhibited.

Key words: photodynamic therapy, Ehrlich ascites tumor, key targets

INTRODUCTION

Nowadays modern cancer treatment is a reasonable combination of several modalities (1–2). Such approach, as a rule, significantly improves the therapeutic outcome and reduces possible side effects. In order to develop new protocols for combination of PDT with radiotherapy or chemotherapy, it is necessary to identify the cytotoxicities induced by each treatment separately, because this knowledge may add valuable information in planning the multimode treatment. Moreover, to understand the mechanism of interaction of different combined treatments (synergistic or additive) it is important to examine not only lethal cell damages, but also sublethal injuries which in combination with other treatments might transfer to lethal and notably increase the therapeutic outcome.

In this study, the main interest is focused on the key targets of photosensitization in EAT cells.

Corresponding author: Živilė Lukšienė, zivile@loc.lt

MATERIALS AND METHODS

Chemicals

The stock solution of hematoporphyrin dimethyl ether (HPde) (gift from Prof. G. V. Ponomarev, Russia), was prepared in physiological saline ($2.5 \times \times 10^{-3}$M) and stored in the dark below 10 °C.

All regents for determination of enzyme activities were obtained from Sigma or Serva.

[^{3}H–6] Thy was obtained from Chemapol (Czech Republic); the other chemicals used for evaluation of DNA synthesis were of highest quality.

Objects

Murine Ehrlich ascites tumor (EAT) model was used for investigations (for a more detail description, see (3)).

Irradiation

The light source for irradiation of EAT cell suspension consisted of tungsten lamp (500 W), optical

system for light focusing, and optical filter for UV and infrared light elimination (370 nm < λ > > 680 nm). Light intensity at the position of the cells was 50 mW/cm^3 and the irradiation time 90 s.

Ehrlich ascites carcinoma (EAT) was transplanted into female mice aged 6–7 weeks and weighing approximately 21 g. The implantation procedure is summarized as follows: a tumor is dissected from a donor mouse and EAT cells (0.8×10^6) as a cell suspension is inoculated intraperitoneally (i. p.) to healthy mice with a 25 G needle (4).

Experimental design

On the 7th day after EAT tumor inoculation in its exponential growth phase, the sensitizer was injected i.p. (10–60 mg/kg of body weight). After 3 h of incubation EAT cells were excluded from the intraperitoneum and prepared *ex vivo* in the dark as a homogeneous cell suspension with the optical density OD (λ = 590 nm) = 0.6 (3.7×10^6 cells/ml). Irradiation of cells was performed in 2 mm cuvettes. After treatment, 0.2 ml of irradiated suspension (0.8×10^6 cells) was inoculated in healthy mice (i.p.). Tumor growth kinetics was measured for 15 and more days. All experiments were done in the dark and repeated 3 times.

Tumor growth determination

Relative Ehrlich ascites tumor growth was measured every day up to day 15 of its growth according to the equation:

$$S = (S_1 - S_0)/S_0,$$

where S_1 is the final weight of the mouse with tumor, S_0 is the initial weight of the mouse, S is relative tumor growth.

Moreover, Ehrlich ascites tumor growth was measured in two other ways:

1. Absolute tumor volume (cm^3) growth for 15 days.
2. Tumor cell number (mill.) for 15 days (5).

The correlation between absolute tumor weight and relative tumor growth was found to be very strong (r^2 = 0.98). In order to simplify the experimental protocol, we usually measured only relative tumor growth.

All animals were under general anesthesia (ketamine hydrochloride, i.p.) during all experiments.

Plasma membrane integrity

Following each irradiation, equal aliquots of Trypan blue (1%) and irradiated cell suspension (3.7 mill./ml) were mixed. After Trypan blue addition cells were counted on a hemocytometer. The percentage of cells excluding Trypan blue was determined as nonstained and divided by the total cell count.

Localization of photosensitizer

For intracellular porphyrin localization in Ehrlich ascites tumor cells, fluorescence microscopy (Lumam Pz (Poland)) was performed. For HPde fluorescence, an ΦCI excitation filter (360–420 nm, Russia) was used. Red fluorescence of intracellular HPde excited by blue light was observed.

EAN cycle analysis

Tumor cell suspensions were centrifuged and resuspended in phosphate-buffered saline (PBS) to a concentration of 10^6 cells/ml. For FACS analysis, cells were stained with 50 μg/ml ethidium bromide in PBS. The DNA analysis of tumor cell populations was performed on a Becton Dickinson FACS flow cytometer with an excitation wavelength of 488 nm and emission above 580 nm. The cell cycle analysis was performed using Cell Fit software. 15,000 cells were analyzed in each experiment (5).

Apoptosis detection in EAT cells

It was evaluated by two methods. Two hours after treatment, nonpermeabilized cells (10^6 cells) were incubated with 4 μg/ml ethidium bromide in a culture medium for 15 min at room temperature, in the dark as described in Ferlini et al. (6). The samples were analyzed with a FACSort instrument (Becton Dickinson). Apoptotic cells were detected on an FSC/FL2 dot plot as an EB (ethidium bromide)^{dim} area. As a negative control, a sample with alive cells was used. Orange/red fluorescence of EB was collected through at 585/42 nm bandpass. Up to 10,000 cells were analyzed using the Lysis II program. Apoptotic and necrotic cells were detected on FCS/FL2 dot plot: R1 area – necrotic, R2 – apoptotic, R3 – viable (7).

Quantification of the apoptotic index was also evaluated by fluorescence microscopy (Nicon), which was based on acridine orange/ethidium bromide uptake in the cells (8)

Measurements of intracellular concentration of photosensitizer in tumors

Ehrlich ascites tumor cells were collected from the mice 3 h after treatment with a photosensitizer. They were suspended in phosphate-buffer solution (PBS) to an optical density OD = 0.6. The fluorescence of the suspension was measured with an SFR-1 epi-

spectrofluorimeter (Russia) at λ = 600–680 nm. An EAT suspension treated in the same manner without photosensitizer was taken as control. Standard curves were produced by adding a known amount of the photosensitizer (9).

Protein quantitation determination in tumors

The quantation of protein was determined by the Bradford method.

Cell antioxidant system damage

After treatment, the cells were immediately frozen and kept for 24 h before measurement of enzyme activity.

The enzyme activity was determined spectrophotometrically using a Hitachi-557 spectrophotometer, in 0.1 M K-phosphate buffer (pH 7.0) containing 1 mM EDTA and 0.16 mg/ml digitonin, at 25 °C. Various amounts (0.05–0.2 ml) of cell suspension (2.5 mg protein/ml) were diluted by the buffer (total volume, 2.0 ml) and incubated for 10 min in order to achieve cell permeabilization. The activity of antioxidant enzymes was determined according to established methods (10). The activity of catalase (CAT) was determined according to the initial rate of decomposition of 10 mM H_2O_2 ($\Delta\varepsilon_{240}$ = 0.04 nM^{-1} cm^{-1}), the unit of enzyme activity expressed as μmol substrate/min × mg. The total activity of CuZn- and Mn-superoxide dismutase (SOD) was determined according to the inhibition of reduction of nitrotetrazolium blue (0.1 mM) by xanthine oxidase and hypoxanthine (1.0 mM), monitored at 560 nm. The unit of enzyme activity was expressed as the amount of protein inhibiting the reaction by 50%. The activity of glutathione reductase (GR) was determined according to the rate of oxidation of 0.1 mM NADPH ($\Delta\varepsilon_{340}$ = 6.2 M^{-1} cm^{-1}) by 1.0 mM oxidized glutathione (GSSG), the unit of enzyme activity expressed as nmol substrate/min × × mg. The acitivity of glutathione-S-transferase (GST) was determined according to the rate of conjugate formation ($\Delta\varepsilon_{340}$ = 9.0 mM^{-1} cm^{-1}) between 2,4-dinitrochlorobenzene (0.1 nM) and 5.0 nM reduced glutathione (GSH). The unit of enzyme activity was expressed as nmol substrate/min × mg. The dark inhibition of GST by Hpde was studied in analogous conditions, except that 12.5–50 μM Hpde was present in the solution.

The photosensitized inactivation of GST by Hpde was studied as follows. A suspension of Ehrlich cells (2.5 mg/ml) in buffer solution with digitonin was incubated with 25 μM Hpde in the dark for 30 min. Later the mixture was irradiated at 25 °C with red light (>590 nm, 25 W/m^2), and the aliquots were taken for GST activity determination at various time intervals.

Evaluation of DNA synthesis

Briefly, the level of DNA synthesis was evaluated as an incorporation of [^{3}H-6] Thy according to (11). 2 μCi/ml of [^{3}H-6] Thy was added to a 2 ml suspension of EAT cells (× 10^x/ml for 30 min at 37 °C. The medium was removed by centrifugation (5 min, 1000 g) the and cells were twice washed with ice-cold PBS. The cells suspended in 2 ml ice-cold PBS were transferred to Millipore GS 0.22 μm filters and washed with PBS. Then the filters were exposed to 5 ml 5% trichloroacetic acid (TCA) for 10 min at 4 °C. The TCA solution was filtered through the same filter. The radioactivity on the filters which corresponded to the amount of [^{3}H-6] Thy incorporated into DNA was measured in toluene scintillation liquid (0.4 g PPP, 0.2 g POPOP in 1l g of toluene) with an LS-100C radiospectrometer (Beckman).

RESULTS

1. EAT growth inhibition after HPde-based PDT in EAT

In order to provide information useful for the further investigation of possible sites of damage in the EAT cells induced after PDT, we have evaluated the dependence of tumor growth inhibition on the HPde concentration applied.

Data presented in Fig. 1 clearly show that in the control not treated group tumor growth was increasing up to day 15 in an exponential mode and reached 0.6 (relative unit). Neither light alone nor HPde had a significant influence on tumor growth. However, after photosensitization tumor growth diminished very no-

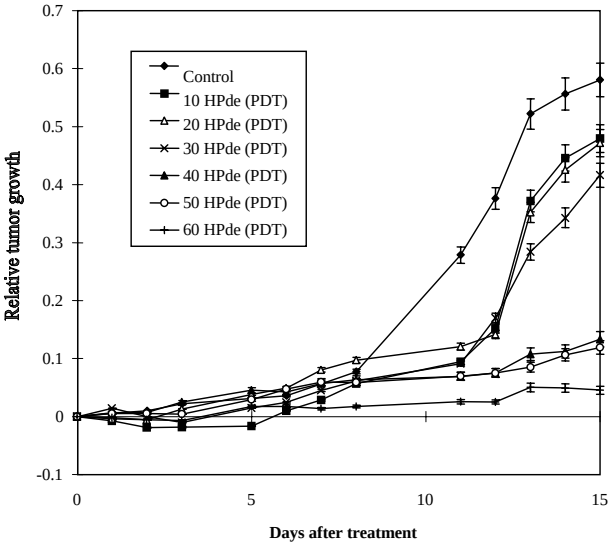

Fig. 1. EAT growth inhibition as function of Hpde concentration used for PDT

tably (from 0.6 to 0), and this effect strongly depended on the HPde concentration applied.

2. Evaluation of the intracellular HPde concentration

In order to be sure that the observed effects depend on HPde concentration, the amount of intracellularly accumulated drug was determined. Due to the fact that all photosensitizers exhibit fluorescence, we used fluorimetric technique to measure their cellular accumulation. The use of epi-fluorimeter was considered as more advantageous in comparison to fluorescence measurements of chemically extracted photosensitizers, because it gives the possibility to evaluate the intracellular concentration of any photosensitizer in intact cells. The data obtained are presented in Fig. 2.

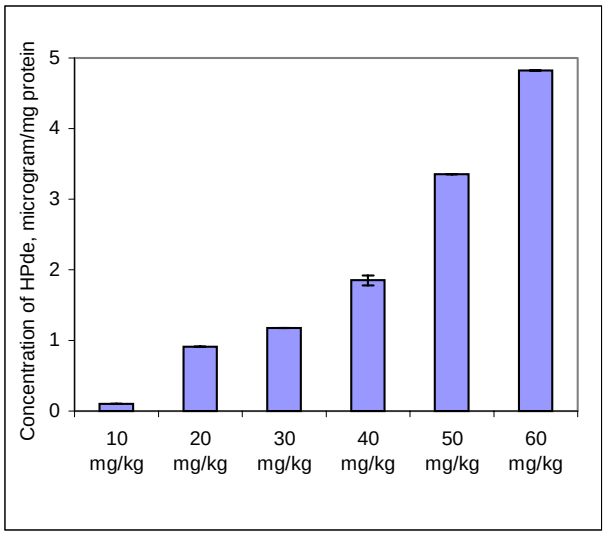

Fig. 2. Intracellular Hpde concentration in EAT cells as function of the concentration of i. p. applied sensitizer

One can see that the higher extracellular concentration of HPde was used, the higher intracellular concentration was obtained. No saturation in this concentration range was observed.

3. Intracellular localization of the photosensitizer

Having determined the accumulation capacity of Hpde in EAT cells, we sought to evaluate the intracellular localization of the photosensitizer. It seems of crucial importance, because, due to the fact that $^1O_2$ cannot migrate far, the sensitizer localization pattern is usually the site of PDT induced damage (12). Hence, in our experimental conditions a fluorescing photosensitizer was usually localized in the plasma membrane, since a bright ring of fluorescence was seen on the outer limits of the cell. Just a weak diffuse fluorescence was observed in the cytosol, mostly in the perinuclear region.

4. PDT effects on cell membrane

As HPde is mostly localized in the cell membrane, it appears of particular interest to study the immediate events induced after HPde-PDT.

Data presented in Fig. 3 indicate that drastic rearrangements of cell membrane are induced after PDT.

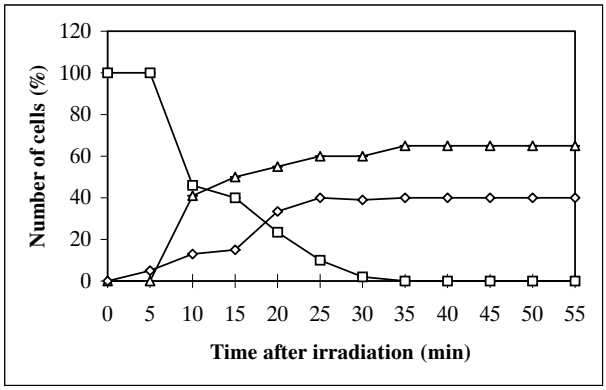

Fig. 3. Immediate desintegration of EAT cell membrane following Hpde-PDT

Immediately after HPde-PDT treatment, cells developed extensive “blebs” on their surface apparently due to extension of the plasma membrane. Figure 3 shows the percentage of “blebbing” cells as a function of time after treatment. It is evident that remarkable damage of cell membrane is the first site of PDT action.

5. PDT effect on antioxidant systems in the cell

Changes in the activities of antioxidant enzymes during photosensitized irradiation may play an im-

Table 1. **Changes in antioxidant enzyme activities after different treatment of EAT cells (U/mg). Statistically significant differences, if any, are given against control values**

Enzyme	Control	HPde-PDT
Catalase	1.57 ± 0.28 n = 5	2.23 ± 0.22 n = 3
Superoxide dismutase	5.84 ± 0.55 n = 5	7.16 ± 2.0 n = 3
Glutathione reductase	31.7 ± 3.0 n = 6	32.8 ± 2.2 n = 3
Glutathione-S-transferase	76.5 ± 10.8 n = 5	15 ± 2.0 n = 4
DT-diaphorase	2.5 ± 0.3 n = 4	<1.0 n = 3

portant role in modulating cell viability. However, these data are not numerous (13, 14).

The data of Table 1 show that the dark treatment of Ehrlich cells by HPde and subsequent irradiation did not result in statistically significant changes in the activities of antioxidant enzymes CAT, SOD, and GRD. Interestingly, the dark treatment by Hpde decreased the activity of glutathione-S-transferase and DT-diaphorase, which were further suppressed by subsequent irradiation.

6. PDT effect on DNA synthesis

The intensity of DNA synthesis in the cell might also reflect a lot of injuries related to the important elements of cell growth and proliferation.

Data presented in Table 2 indicate that DNA synthesis in EAT cells after Hpde-PDT is really a very sensitive process.

Table 2. **Effect of Hpde-PDT on DNA synthesis. Statistically significant differences, if present, are given against control values.**
♦ – incorporation of [^{3}H]Thy into DNA of control cells was equated as 100%.
♣ – the DNA synthesis level was calculated as % of control cell synthesis level

	Control (♦,%)	HPde + PDT (♣,%)
Synthesis level measured after 18–20 h of treatment	100 ± 5.0 n = 5	27.5 ± 4.5 n = 4
Synthesis level measured after 3–5 h of treatment	100 ± 5.0 n = 3	32.0 ± 5.0 n = 3

The results presented in Table 2 suggest that HPde-PDT treatment drastically reduces the rate of DNA synthesis (27.5% of the control level). These data correlate well with the results obtained further analyzing cell division and cell death pathways induced by photosensitization.

7. PDT effect on the cell-cycle distribution

On the basis of previous studies, it appears of particular interest to determine if there is some influence of the above-mentioned damages on cell cycle. Data presented in Fig. 5A can clearly indicate that control cells were with the dominant subpopulation in G_0/G_1 phase, whereas cells following 24 h after PDT treatment exhibited a diminished G_0/G_1 and a slight increase in S and G_2M phase. Moreover, there are much less cells in the cycle, what means that some of them are dead.

It is clear from Fig. 5B that an increase of HPde concentration from 30 mg/kg to 60 mg/kg makes a more significant depletion of G_0/G_1 and accumulation of cells in S and G_2M phases.

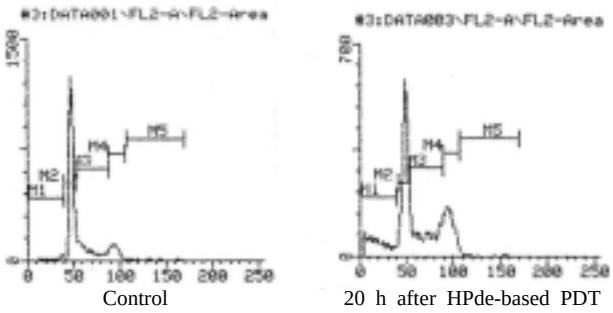

Fig. 5A. EAT cell-cycle redistribution after Hpde-based PDT. DNA histogram: M_1 – dead cells; M_2 – G_0/G_1; M_3 – S; M_4 – G_2M

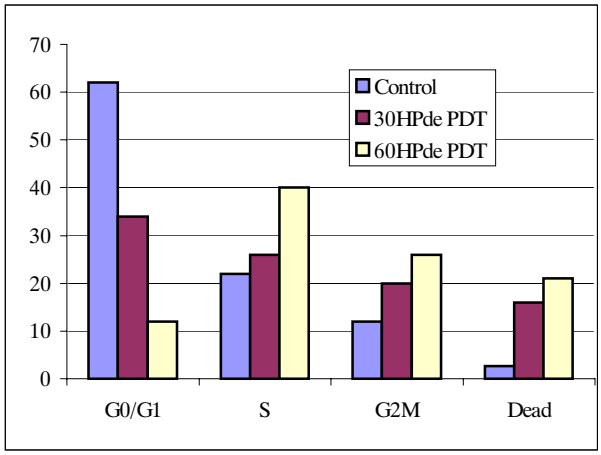

Fig. 5B. EAT cell-cycle dependence on Hpde dose used for PDT

8. PDT effect on cell death pathways

Cell death pathways induced after PDT usually are necrosis or apoptosis. We investigated EAT cell death pathways after PDT treatment using a flow-cytometric technique. Here we will report also some experiments carried out to elucidate certain aspects of apoptosis induction.

First of all, we tried to detect early signs of apoptosis 2 h after PDT treatment. Figure 6 shows the percentage of EAT cells (alive, apoptotic, necrotic) after PDT. One can se that the control cell population consisted of 90% alive cells, and the increasing concentration of HPde (30HPde(+)), (60HPde(+)) did not change the viability of the population, whereas cells after PDT (30 PDT+) exhibited a drastic decrease in viability (just 35% alive), and new subpopulations of apoptotic (25%) as well as necrotic (25%) cells appeared. Afterwards we examined the dependence of the way of cell death af-

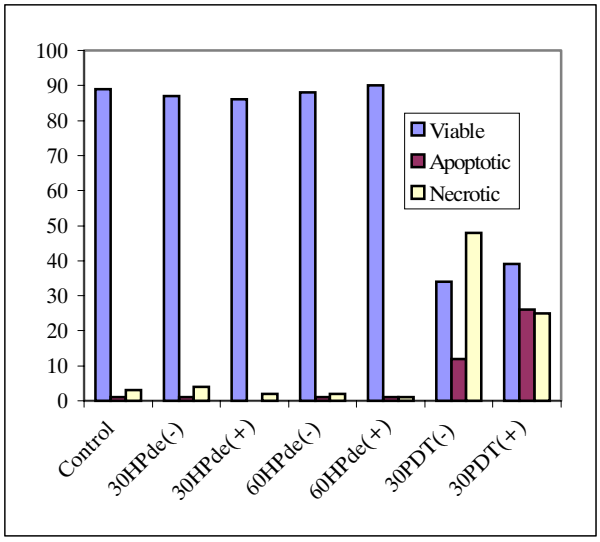

Fig. 6. Percentage of alive/apoptotic/necrotic EAT cells 2 hours following Hpde-PDT treatment

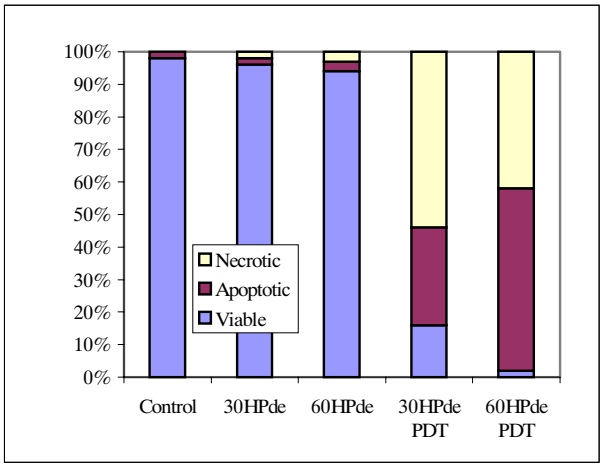

Fig. 8. Development of apoptotic process in EAT cells 20 h after HPde-PDT treatment

ter PDT on experimental conditions. In the first case, cells were kept 2 h after treatment in PBS (starving conditions) and in the second case in RPMI medium (physiological conditions). This shows that not treated cells (30 HPde(–), 30 HPde(+)) did not depend on nutrition during 2 h and the percentage of alive, necrotic and apoptotic cells did not change. On the contrary, cells that underwent PDT treatment strongly depended on nutrition: cells incubated in PBS (30PDT (–)) exhibited a much more necrotic subpopulation (45%), whereas cells incubated in medium (30 HPde (+)) were undergoing in parallel necrosis (25%) and apoptosis (25%).

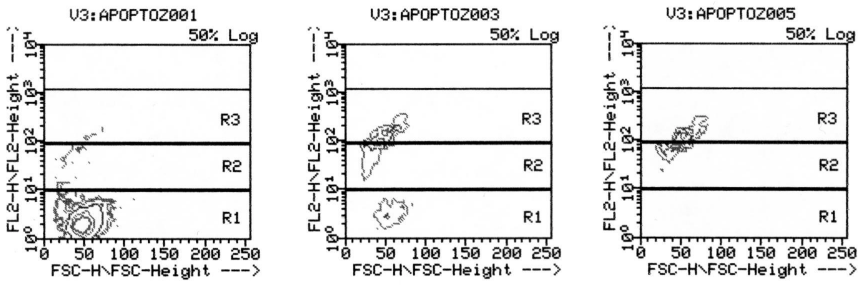

a) Control b) 30 HPde-PDT c) 60 HPde-PDT

Fig. 7. Apoptosis induction in EAT cells 20 h after HPde-PDT: a – control, b – 30 mg/kg HPde-PDT, c – 60 mg/kg HPde-PDT. R_1 gate – alive cells, R_2 gate – apoptotic cells, R_3 gate – necrotic cells

Considering these observations, we further investigated how cell death depended on the time after PDT treatment. Figure 10 and Fig. 8 indicate that after 20 h the control cells remained the same (alive), 30 HPde- or 60 HPde-treated cells did not differ from control, whereas 30 HPde-PDT- or 60 HPde-PDT treated cells showed a reduction in alive cell subpopulation and a remarkable increase in necrotic and apoptotic cell subpopulations.

As stated above, usually most of HPde-PDT-treated EAT cells after 20 h are apoptotic or necrotic, and just the minority of them is alive. Coming back to the cell cycle data would help us to understandin what phase cells are dying. Figure 5A clearly shows that depletion of G_0/G_1 might indicate that the cell death and especially apoptosis is induced from G_0/G_1 phase of the cell cycle. By the way, these data are in line with the worldwide accepted opinion that apoptosis is induced from G_0/G_1 phase (15). An increased "HPde dose" (60HPde PDT) diminished the accumulation of cells in G_0/G_1 more significantly than did 30 HPde PDT, mostly because at higher HPde concentrations more intensive photosensitization and subsequently more extensive apoptosis is induced.

DISCUSSION

It is evident from the above-presented data that HPde after i.p. injection reaches the ascite tumor cells, accumulates mostly in cell membrane and after photosensitization inhibits tumor growth.

Moreover, tumor growth inhibition is directly related to the HPde concentration applied. It is necessary to note that the HPde concentrations used (10–60 mg/kg body weight) after intracellular delivery have been found to be very close to those usually applied for PDT (~pg/cell,

~ μg/mg protein (19)). Thus, it seems possibl that the first target of damage in the cell after HPde-PDT is cell membrane. The immediate increase of the number of blebbing cells parallelly with the decrease of viable cells is the best evidence of it. The following investigation of he activities of the antioxidant enzymes CAT, SOD, GRD clearly indicates that an oxidative stress takes place.

It is interesting to note that oxidative stress did not result in changes of CAT, SOD, GRD activities – just glutathione-S-transferase was inhibited after photosensitization.

It has been shown previously [14] that the activities of CAT and SOD after photosensitization of mouse mammary carcinoma cells in the presence of hypericin transiently increased (up to 200% after 0.5–1.0 h), but further, depending on the conditions of experiment, dropped close to or slightly above the control levels. Our data show that HPde-PDT exerts analogous effects. In the oxidative stress conditions there was no impact on the activity of glutathione reductase (Table 1). Thi is in contrast to our previous observations in a cell-free system, where glutathione reductase was photoinactivated in the presence of hematoporphyrin and Al-phthalocyanine tetrasulfonate ($T_{1/2}$ = 20–30 min), whereas CAT and SOD were not inactivated [Kliunkienė, 1996]. Evidently, intracellular GRD was protected by intracellular antioxidants such as GSH, which has been shown by our studies in a cell-free system [Kliunkienė, Juodka, 1987].

It is commonly accepted that oxidants, *e.g.*, H_2O_2, activate the antioxidant response element, which acts as a promoter of genes of several xenobiotic-detoxifying enzymes, including DT-diaphorase and glutathione-S-transferase (8). Thus, one may expect an increase in glutathione-S-transferase activity under photosensitization. In any case, the observed decrease in GST activity under the action of HPde-PDT deserves further interest in combinations of photodynamic therapy or radiotherapy with chemotherapy, since it may increase the cell sensitivity to alkylating agents.

Further investigations of EAT cell cycle redistribution induced after HPde-PDT clearly show a significant arrest of the cells in S G_2M phase. This might be easily explained by the injuries of mitotic apparatus (17). Besides, a remarkable depletion of G_0/G_1 phase might indicate that cell death is initiated from the G_0/G_1 phase. It is understandable that under oxidative stress conditions induced after HPde-PDT, DNA synthesis in the cells is inhibited. The subsequent step of cell death pathways analysis supported the idea that the following plethora of damages induced in EAT cells after photosensitization, the cell suicide program is activated. An immediate apoptotic process was detected in HPde-PDT-treated EAT cells parallelly with necrotic. It would therefore be reasonable to assume that necrotic as well as apoptotic processes take place after photosensitization, the apoptotic process strongly depending on experimental conditions and easily modifiable. Moreover, apoptosis develops in time and following 20 h after treatment apoptotic cell subpopulation is much larger than after 2 hs (30% and 10%).

The overall findings of this study allow us to conclude that the key targets of HPde-PDT in EAT cells are cell membranes, induced oxidative stress, following arrest of cell cycle, inhibition of DNA synthesis and eventually fast apoptosis or necrosis. Taking all these considerations into account, it is clear that after photodynamic action the loss of cell integrity, normal functions and viability result from a critical damage of the important cellular targets understanding of which might remarkably simplify the development of new combined treatment protocols in clinics.

ACKNOWLEDGEMENTS

Authors would like to thank L. Rutkovskienė for technical assistance and Dr. D. Characiejus for help in the interpretation of the flow-cytometrical data.

This study was financially suported by the Lithuanian State Science and Studies Foundation.

Received 15 April 2002
Aceepted 10 September 2002

References

1. McCaughan JS. Photodynamic therapy. Drugs and Aging 1999; 15 (1): 49–68.
2. Kalka K, Merk H, Mukhtar H. Photodynamic therapy in dermatology. J Am Acad Dermatol 2000; 42(3): 389–414.
3. Luksiene Z, Juodka B. Porphyrins as radiosensitizers in ^{60}Co irradiated Ehrlich ascites cells: possibility to combine ^{60}Co irradiation with PDT. Proceedings of SPIE, Los Angeles 1993: 67–75.
4. Luksiene Z, Atkocius V, Juodka B. Radiosensitization by porphyrins in ^{60}Co irradiated cells of different nature. Proceedings of Basic Applications of Lasers 1994; 2078: 447–9.
5. Luksiene Z, Kaspariunaite G, Aleknavicius E, Valuckas K. Enhancement of photosensitization effivciency by various combinations with radiosensitization in an experimental Ehrlich ascites tumor. SPIE, Photochemotherapy; PDT and other modalities 1996; 2924: 252–8.
6. Ferlini C, Cesare S, Rainaldi S, Halorni W, Samoggia P, Biselli R, Fattorossi A. Flow-cytometric analysis of early phases of apoptosis by cellular and nuclear techniques. Cytometry 1996; 24: 106–15.

7. Luksiene Z, Kalvelyte A, Supino R. On the combination of photodynamic therapy and ionizing radiation. J Photochem Photobiol 1999 a; 52: 35–42.
8. McGahon AJ. Methods for the study of apoptosis *in vitro*. Meth Cell Biol 1995; 46: 153–85.
9. Luksiene Z, Rutkovskiene L, Jurkoniene S, Maksimov G, Griciute L. Evaluation of the photobiological efficiency of $TPPS_4$ in two different types of mice tumors. Acta Medica Lituanica 2002; 9: 32–6.
10. Habig WH, Pabst MJ, Jakoby WB. Glutathione-S-transferases. J Biol Chem 1974; 249: 7130–9.
11. Berg K, Moan J Photodynamic effects of Pii on cell division in human NHIK 3025 cells Int J Radiat Biol 1988; 53: 797–811.
12. Moan J. Porphyrin photosensitization and phototherapy. Photochem Photobiol 1986; 43: 681–90.
13. Kliukiene R, Maroziene A, Cenas N, Becker K, Blanchard JS. Photoinactivation of trypanothione reductase and glutathione reductase by Al-phtalocyanine tetrasulfonate and hematoporphyrin. Biochem Biophys Res Commun 1996; 218: 629–32.
14. Johnson SAS, Pardini RS. Antioxidant enzyme response to hypericin in EMT6 mouse mammary carcinoma cells. Free Rad Biol & Med 1998; 24: 817–26.
15. Darzynkiewicz JS, Li X, Gorczyca W et al. Cytometry in cells necrobiology: analysis of apoptosis and accidental cell death (necrosis). Cytometry 1997; 27(1): 1–20.
16. Kliukiene R, Maroziene A, Nivinskas H, Cenas N, Kirveliene V, Juodka B. The protective effects of dihydrolipoamide and glutathione against photodynamic damage by Al-phthalocyanine tetrasulfonate. Biochem Mol Biol Int 1997; 41: 703–17.
17. Berg K, Moan J, Bommer JC, Winkleman JW. Cellular inhibition of microtubule assembly by photoactivated sulfonated tetraphenylporphyrines. Int J Radiat Biol 1990; 58: 475–87.
18. Li Y, Jaiswal AK. Regulation of human NAD(P)H: quinone oxidoreductase gene. J Biol Chem 1992; 267: 15097–104.
19. Miyoshi N, Hisazumi H, Ueki O, Nakajima K, Fukuda M. Photodynamic inactivations of cultivated human bladder cancer argon-dye laser light. Photobiochem Photobiophys 1985; 9: 241–52.

Ž. Lukšienė, D. Labeikytė, A. Marozienė, R. Kliukienė, N. Čėnas, B. Juodka

EHRLICHO ASCITINIO NAVIKO PAŽEIDIMO MECHANIZMAS PO FOTODINAMINĖS TERAPIJOS

S a n t r a u k a

Darbe buvo nustatyta Ehrlicho ascitinio naviko augimo inhibicija po HPde fotoindukuoto poveikio. Tirtos visos galimos FDT sukeltos pažaidos. Pastebėta, kad iš karto po FDT poveikio vyksta membranų dezintegracija, oksidacinis stresas, DNR sintezės inhibicija, ląstelės ciklo stabdymas S ir G_2M fazėse bei apoptozės ir nekrozės procesų aktyvizacija. Įrodyta, kad apoptozė ląstelėje vyksta aktyviai, ir jos metu sunaudojama energija. Nesant energijos šaltinio, apoptozė ląstelėje transformuojasi į nekrozę. Nustatyta, kad EAN ląstelėse apoptozė indukuojama esant joms G_0/G_1 fazėje.